Обзор ArXiv/astro-ph, 23-27 ноября 2020

От Сильченко О.К.

ArXiv: 2011.11629

Bulge formation through disc instability - I. Stellar discs

T. Devergne[1], A. Cattaneo[2,3], F. Bournaud[4], I. Koutsouridou[2], A. Winter[5], P. Dimauro[6], G. A. Mamon[3], W. Vacher[7], and M. Varin[7]

[1] Université Paris XI, 91405 Orsay, France
[2] Observatoire de Paris/LERMA, PSL University, 61 av. de l'Observatoire, 75014 Paris, France
[3] Institut d'Astrophysique de Paris, CNRS, 98bis Boulevard Arago, 75014 Paris, France
[4] CEA/IRFU/SAp, 91191 Gif-sur-Yvette Cedex, France
[5] Université de Cergy-Pontoise, 33 Boulevard du Port, 95011, Cergy, France
[6] Observatório Nacional do Rio de Janeiro (ON), Rua Gal. José Cristino 77, São Cristóvão, 20921-400 Rio de Janeiro, RJ, Brazil
[7] Observatoire de Paris/GEPI, PSL University, 61 av. de l'Observatoire, 75014 Paris, France

Received — / Accepted —

ABSTRACT

We use simulations to study the growth of a pseudobulge in an isolated thin exponential stellar disc embedded in a static spherical halo. We observe a transition from later to earlier morphological types and an increase in bar prominence for higher disc-to-halo mass ratios, for lower disc-to-halo size ratios, and for lower halo concentrations. We compute bulge-to-total stellar mass ratios B/T by fitting a two-component Sérsic-exponential surface-density distribution. The final B/T is strongly related to the disc's fractional contribution $f_{\rm d}$ to the total gravitational acceleration at the optical radius. The formula $B/T = 0.5 f_{\rm d}^{1.8}$ fits the simulations to an accuracy of 30%, is consistent with observational measurements of B/T and $f_{\rm d}$ as a function of luminosity, and reproduces the observed relation between B/T and stellar mass when incorporated into the GALICS 2.0 semi-analytic model of galaxy formation.

Что будет проверено и улучшено? Критерий устойчивости звездных дисков

Efstathiou, Lake, & Negroponte (1982, ELN) extended the analysis by Combes & Sanders (1981) to the more realistic case of an exponential disc and found a condition for the circular velocity V_c at 2.2 exponential scale-lengths, where the rotation curve of a self-gravitating exponential disc peaks (Freeman 1970). A thin exponential stellar disc embedded in a static spherical DM halo becomes unstable and develops a bar if

$$V_c(2.2R_d) < \epsilon\sqrt{\frac{GM_d}{R_d}}, \qquad (1)$$

where M_d is the disc mass, R_d is the exponential scale-length and $\epsilon = 1.1$. Christodoulou et al. (1995) used analytic arguments to conclude that a similar criterion with $\epsilon = 0.9$ should apply to gaseous discs.

Начальные условия

We assume that the disc is exponential and isothermal in the vertical direction (for example, Villumsen 1985; Efstathiou 2000). These assumptions give the density distribution:

$$\rho(r,z) = \frac{1}{2h}\mathrm{sech}^2\left(\frac{z}{h}\right)\frac{m_\mathrm{d}}{2\pi r_\mathrm{d}^2}e^{-\frac{r}{r_\mathrm{d}}}, \tag{3}$$

where h is disc's vertical scale-length (all quantities in Eq. 3 are adimensional). As our goal is to study the stability of thin discs (discussion in Section 4), we run all our simulations for $h/r_\mathrm{d} = 0.044$. This value is small but not un-

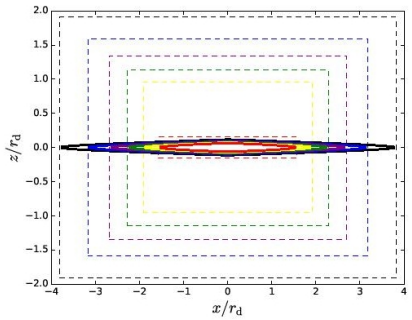

Fig. 1. Initial conditions and refinement regions. The black, blue, violet, green, yellow, and red curves show the isodensity contours that contain 90%, 80%, 70%, 60%, 50%, and 40% of the disc mass at $t = 0$, respectively. The black, blue, violet, green, yellow, and red dashed lines show the cylinders within which the cell size equals 1/8, 1/16, 1/32, 1/64, 1/128, and 1/256 of the disc exponential scale length, respectively.

Stars have velocity dispersion:

$$\sigma^2(r) = \pi h\frac{m_\mathrm{d}}{2\pi r_\mathrm{d}^2}e^{-\frac{r}{r_\mathrm{d}}} \tag{6}$$

determined from Eq. (3) through the requirement that our initial condition should be in equilibrium (albeit unstable). Hence, their velocities:

$$\mathbf{v} = \mathbf{v}_\mathrm{rot} + \Delta\mathbf{v} \tag{7}$$

will be the sum of an ordered rotational component (oriented as $\hat{\mathbf{e}}_\phi$) and a random deviate from a Maxwellian distribution with velocity dispersion σ. The assumption of an isotropic velocity dispersion is motivated by simplicity, but it is not unreasonable, since the radial and vertical velocity dispersions in the Solar Neighbourhood are $(35 \pm 5)\,\mathrm{km\,s^{-1}}$ and $(25 \pm 5)\,\mathrm{km\,s^{-1}}$, respectively (Bland-Hawthorn & Gerhard 2016).

Тонкий экспоненциальный диск в гидростатическом равновесии

Еще:

- Сферическое статическое темное гало
- 2% по массе газа
- Изолированная галактика
- Свободные параметры модели: масса диска m_d (относительно массы гало), радиус диска r_d (= λ /2, относительно вириального радиуса) и концентрация темного гало c.
- Результат расчета: B/T для псевдобалджа!

Результаты эволюции за 2 млрд лет

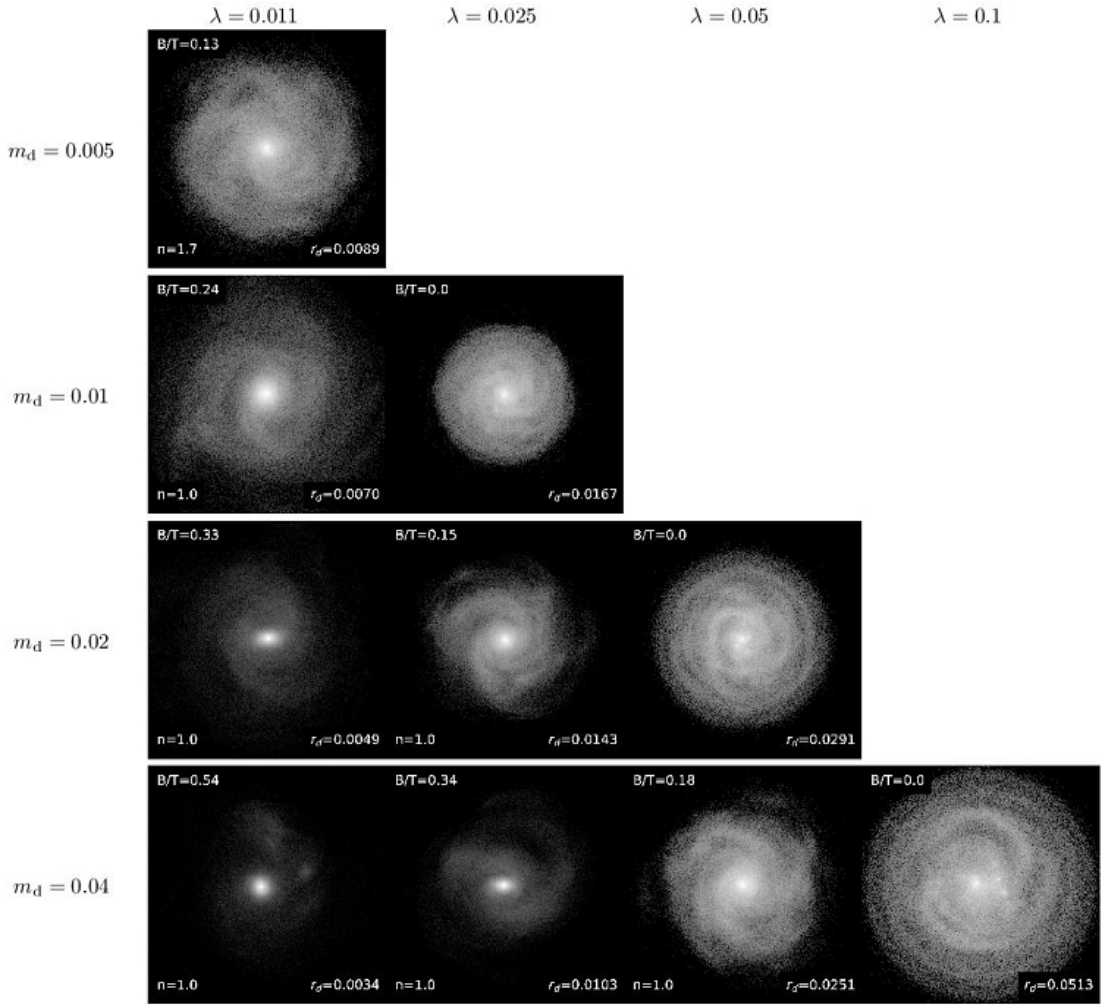

g. 2. Face-on view of the simulated galaxies at the first time t when B/T has stopped growing ($2\,\mathrm{Gyr} < t < 3\,\mathrm{Gyr}$). The age brightness is proportional to the logarithm of stellar surface density. This figure show the simulations with $c = 5$, sorted by

Результаты эволюции за 2 млрд лет

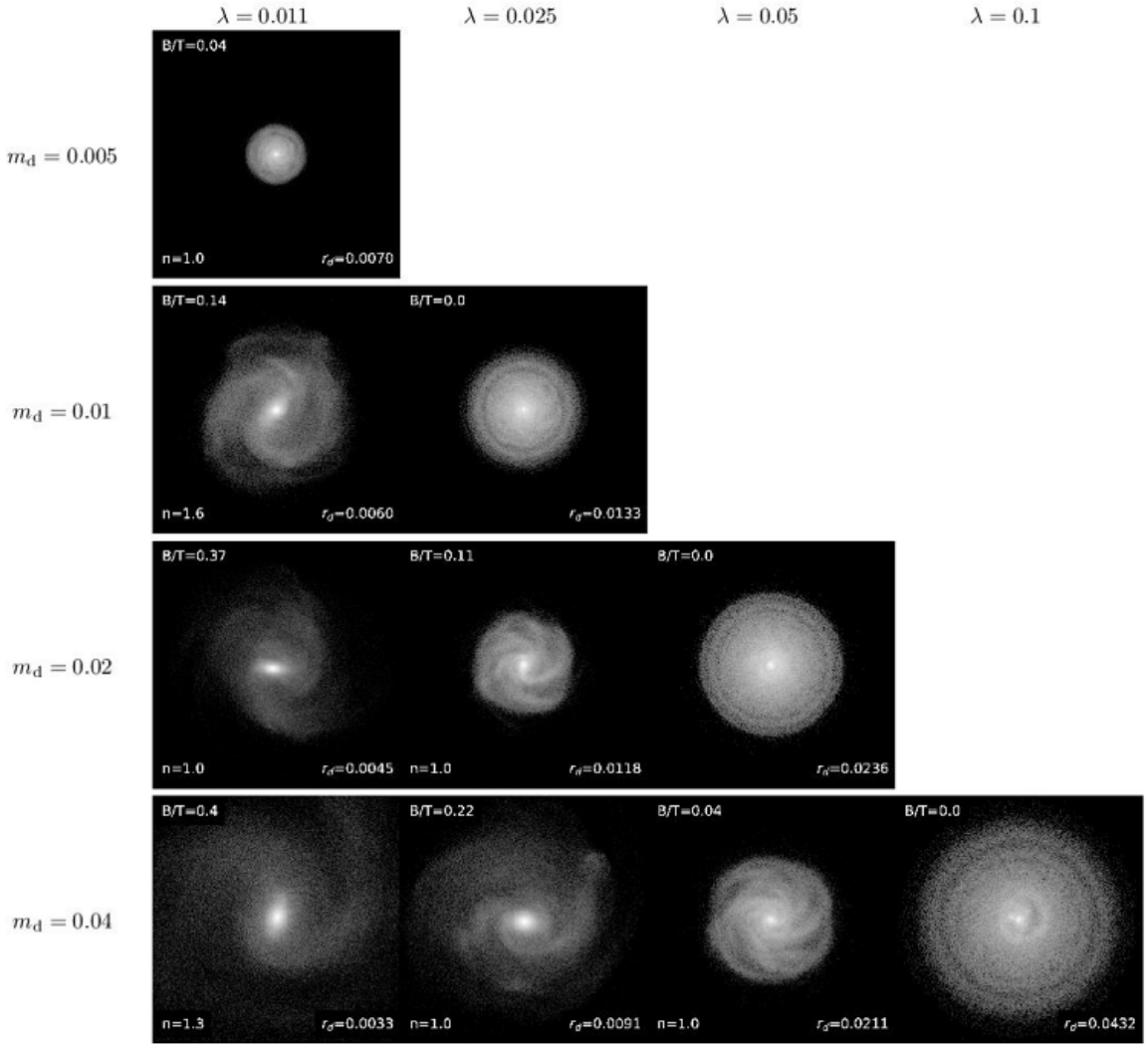

ig. 3. Same as Fig. 2 with $c = 10$ instead of $c = 5$. To avoid overcrowding the figure, we have not shown the simulations with $= 0.018$ and $\lambda = 0.35$

Результаты эволюции за 2 млрд лет

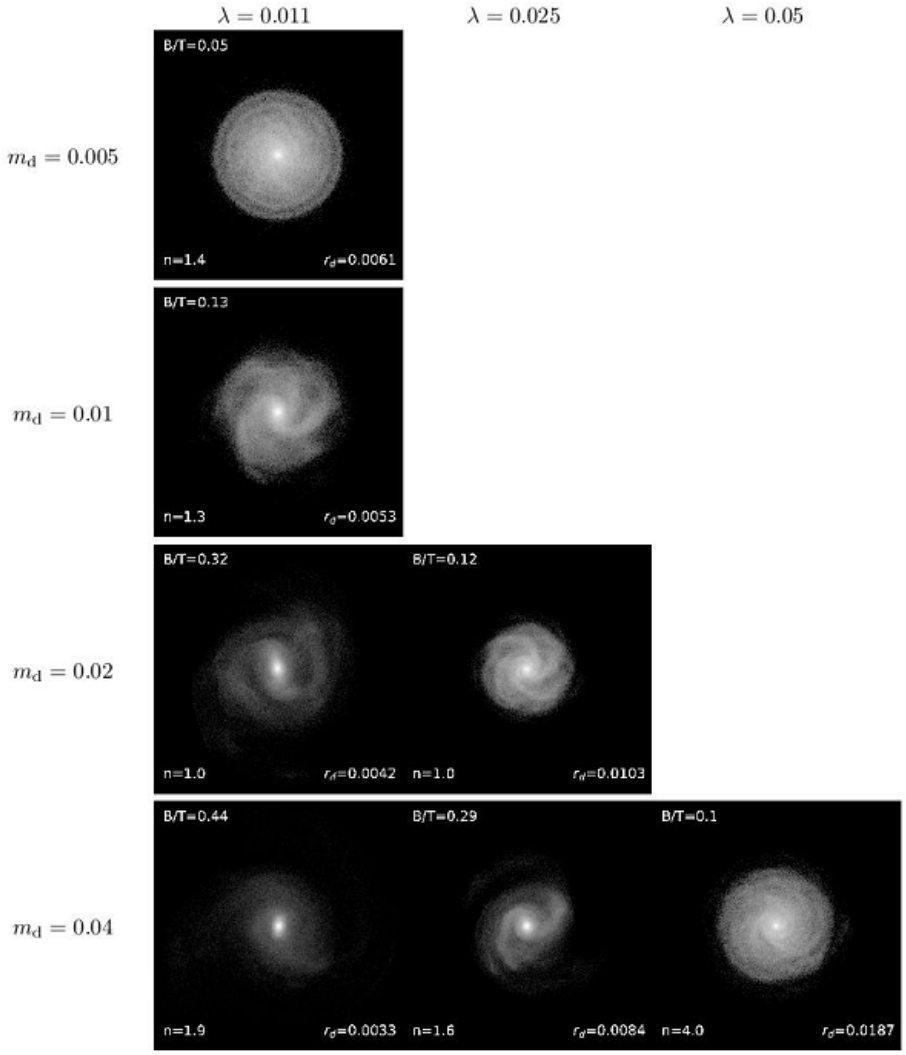

. 4. Same as Fig. 2 with $c = 15$ instead of $c = 5$. The column $\lambda = 0.1$ is now missing because we know that simulations 0.1 will not form any (pseudo)bulge.

Пример – вид сбоку: boxy bulge

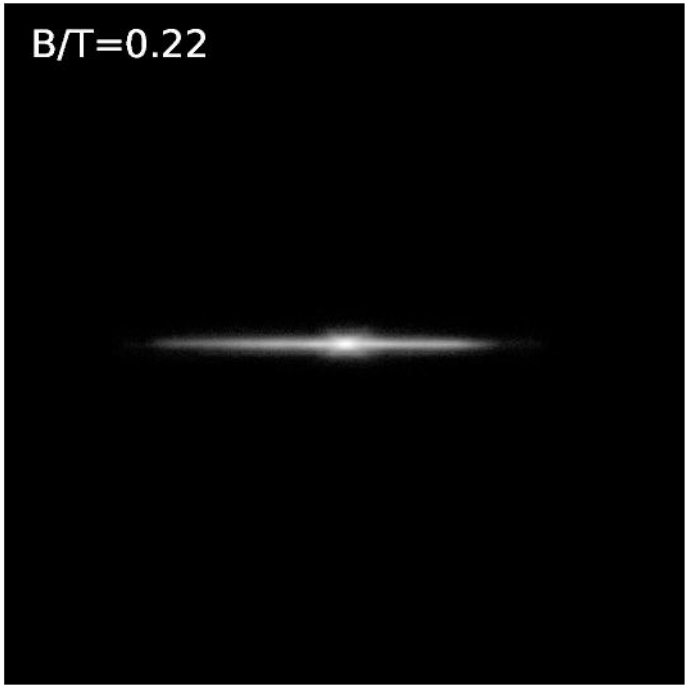

Fig. 5. Galaxy in the simulation with $c = 10$, $m_{\rm d} = 0.04$, $\lambda = 0.025$, viewed edge-on. An X-shaped pseudobulge is clearly visible. This galaxy has been chosen as an example and is by no means atypical. The face-on image (Fig. 3) shows that this galaxy has a bar, but not a prominent one.

Пример: профиль поверхностной плотности с балджем и без

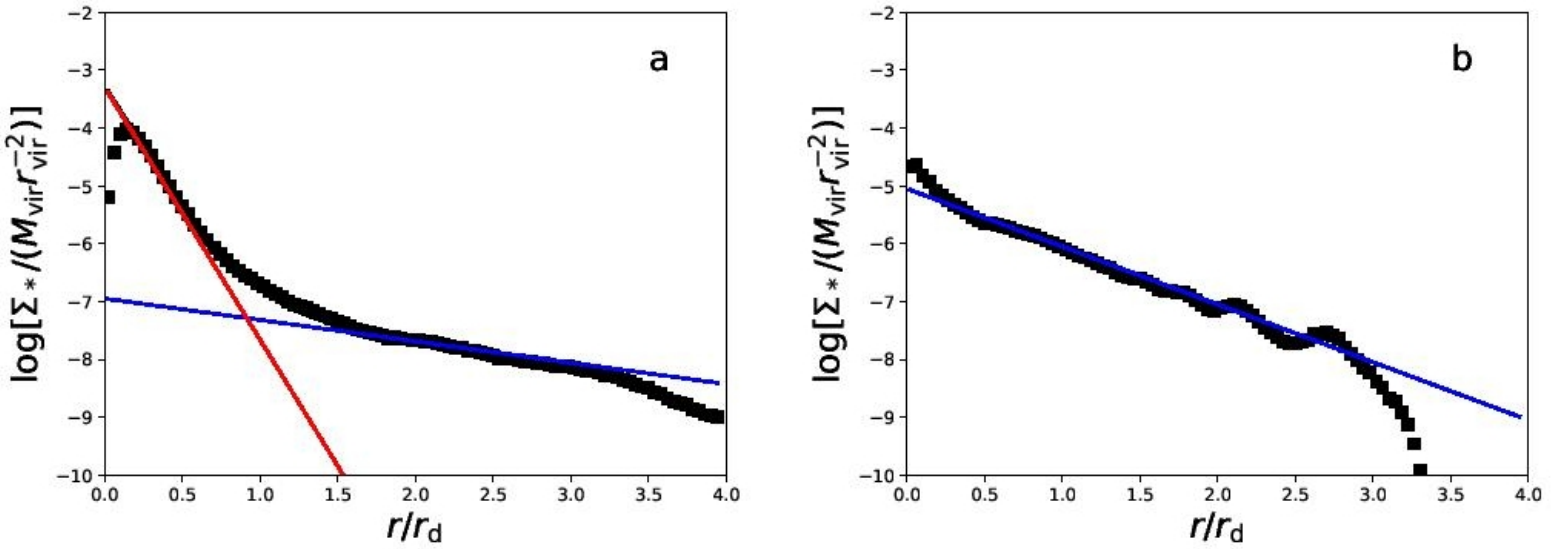

Fig. 6. Stellar surface-density for two of our simulated galaxies (black symbols). Galaxy a has been fitted with the sum of an exponential profile (blue line) and a Sérsic profile, with $n = 1$ in this particular case (red line). Its bulge-to-total mass ratio is $B/T = 0.22$. The black curve shows the sum of the two components. Galaxy b is consistent with a single exponential profile (blue line).

Результат в формулах:

The qualitative findings above have a simple interpretation, which will become apparent once we have examined the ELN criterion in greater detail.

For an exponential disc:

$$v_{\rm d}(2.2r_{\rm d}) = 0.62\sqrt{\frac{m_{\rm d}}{r_{\rm d}}} = \sqrt{1.3\frac{m_{\rm d}(2.2r_{\rm d})}{2.2r_{\rm d}}}, \qquad (12)$$

where $m_{\rm d}(2.2r_{\rm d}) = 0.65m_{\rm d}$ is the disc mass within $2.2r_{\rm d}$ (Freeman 1970). The first equality in Eq.(12) implies that Eq. (1) can be rewritten as:

$$\frac{v_{\rm d}(2.2r_{\rm d})}{v_{\rm c}(2.2r_{\rm d})} > \frac{0.62}{\epsilon}. \qquad (13)$$

By introducing the new parameter $\alpha = 0.31/\epsilon$, Eq. (13) can be written in the alternative form:

$$\frac{v_{\rm d}(2.2r_{\rm d})}{v_{\rm c}(2.2r_{\rm d})} > 2\alpha, \qquad (14)$$

where $\alpha = 0.28$ for $\epsilon = 1.1$ (ELN) and $\alpha = 0.26$ for $\epsilon = 1.2$ (Christodoulou et al. 1995)[4].

The second equality in Eq. (12) shows that Eq. (14) is equivalent to a criterion on the disc fraction within $2.2r_{\rm d}$ because $v_{\rm c}^2(2.2r_{\rm d})/(2.2r_{\rm d})$ is the total gravitational acceleration at $r = 2.2r_{\rm d}$ in dimensionless units and $v_{\rm d}^2(2.2r_{\rm d})/(2.2r_{\rm d})$ is the disc's contribution. Therefore,

$$f_{\rm d}(2.2r_{\rm d}) = \left[\frac{v_{\rm d}(2.2r_{\rm d})}{v_{\rm c}(2.2r_{\rm d})}\right]^2. \qquad (15)$$

is the disc's fractional contribution to the gravitational acceleration at $r = 2.2r_{\rm d}$ and is related to disc's mass fraction

$$f_{\rm d}^{\rm crit} = (2\alpha)^2 \simeq 0.31 \qquad (17)$$

for $\alpha \simeq 0.28$.

The qualitative picture is the same at $r = 2.2r_{\rm d}$ and $r = 3.2r_{\rm d}$. At $f_{\rm d} \ll f_{\rm d}^{\rm crit}$, all galaxies are pure discs (the galaxies with $B/T = 0.01$ in Fig. 7 are bulgeless galaxies; we have assigned them $B/T = 0.01$ merely to be able to show them on a logarithmic plot). At $f_{\rm d} \gg f_{\rm d}^{\rm crit}$, all galaxies develop a pseudobulge and display a tight correlation between B/T and $f_{\rm d}$. At intermediate $f_{\rm d}$, galaxies with $B/T = 0$ and $B/T > 0$ coexist. Therefore, the ELN criterion may fail to discriminate between stable and unstable discs (Athanassoula 2008; Fujii et al. 2018). Nevertheless, the notion of a critical $f_{\rm d}$ that separates the two populations remains fundamentally valid.

Морфология vs доля диска в массе

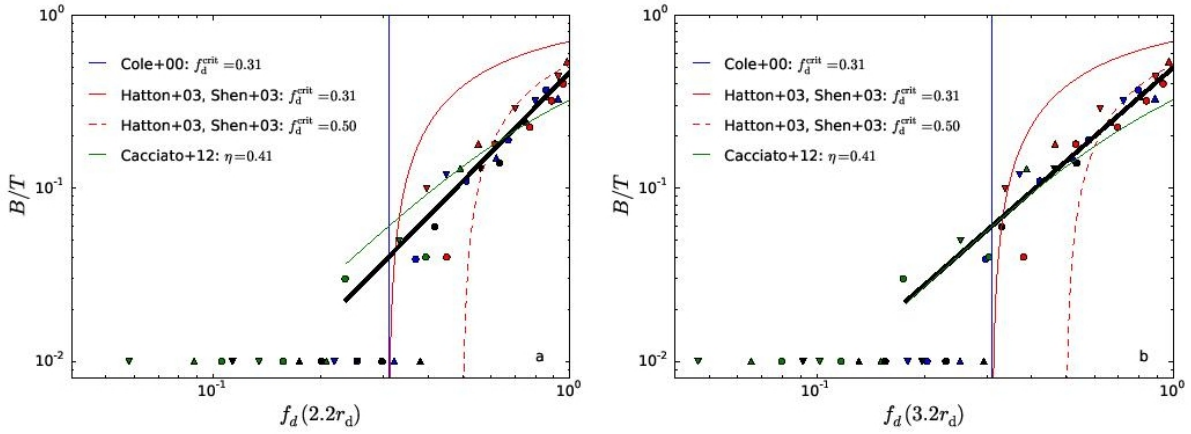

Fig. 7. Relation between bulge-to-total mass ratio B/T and initial disc fraction $f_{\rm d}(r)$ for $r = 2.2r_{\rm d}$ (left) and $r = 3.2r_{\rm d}$ (right). Triangles pointing up, circles, and triangles pointing down correspond to simulations with $c = 5$, $c = 10$, and $c = 15$, respectively. The colours correspond to different disc-to-virial mass ratios: $m_{\rm d} = 0.005$ (green), $m_{\rm d} = 0.01$ (black), $m_{\rm d} = 0.02$ (blue), and $m_{\rm d} = 0.04$ (red). Symbols with $B/T = 0.01$ correspond to bulgeless galaxies. They have been assigned $B/T = 0.01$ merely to be able to show them on a logarithmic diagram. The thick solid black lines are log-log linear least-squares fits to the symbols with $B/T > 0.01$. They correspond to Eqs. (18) and (19). The vertical blue lines show the critical $f_{\rm d}$ that corresponds to the $\alpha = 0.28$ (equivalent to assuming $\epsilon = 1.1$ in Eq. 1) The coloured curves compare our results to previous models (Cole et al. 2000; Hatton et al. 2003; Shen et al. 2003; Cacciato et al. 2012).

If we restrict our attention to galaxies with $B/T > 0$ and apply a linear least-squares fit to the relation between $\log(B/T)$ and $\log f_{\rm d}$, we find:

$$\frac{B}{T} = 0.47 f_{\rm d}^{2.1}(2.2r_{\rm d}) \qquad (18)$$

and

$$\frac{B}{T} = 0.50 f_{\rm d}^{1.8}(3.2r_{\rm d}) \qquad (19)$$

(thick black solid lines in Figs. 7a and b, respectively).

Eq. (18) implies $B/T = 0.04$ for $f_{\rm d} = f_{\rm d}^{\rm crit} = 0.31$. With

Сравнение с наблюдениями – отлично!

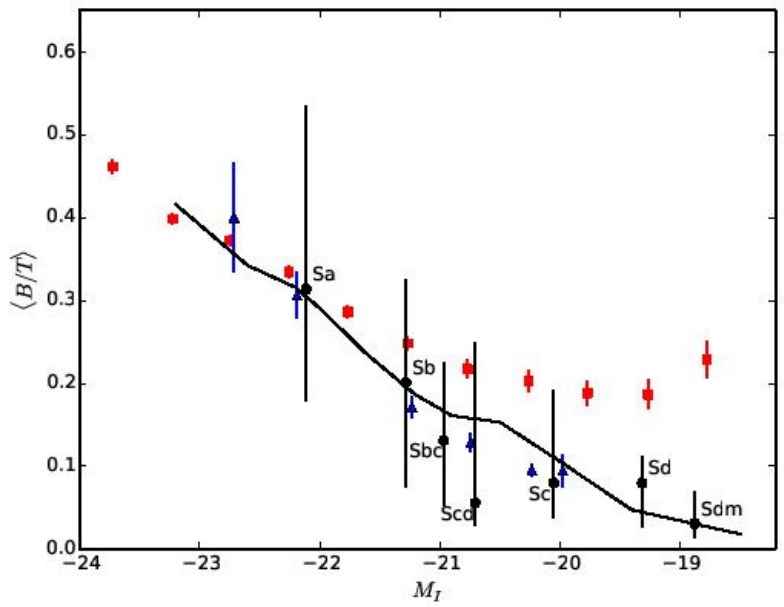

Fig. 8. $\langle B/T \rangle$ versus I-band magnitude M_I. The black curve shows our prediction. The black circles are from Mathewson et al. (1992) when we assign to each Hubble type the $\langle B/T \rangle$ from Graham & Worley (2008; the uncertainty of estimating B/T determines the size of the error bars). The red squares are from Simard et al. (2011) after removing all galaxies with $B/T > 0.7$. The up-pointing filled blue triangles and the down-pointing empty blue triangles are from Salo et al. (2015, S^{4}G) when we assign the bar to the bulge and the disc, respectively.

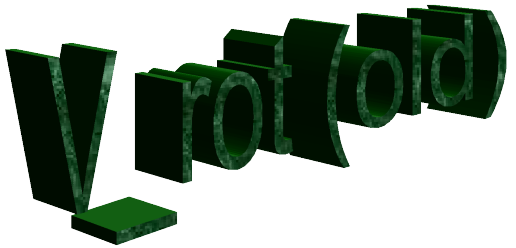

И тут иза-за куста достают SAM=Semi-Analytical Models…

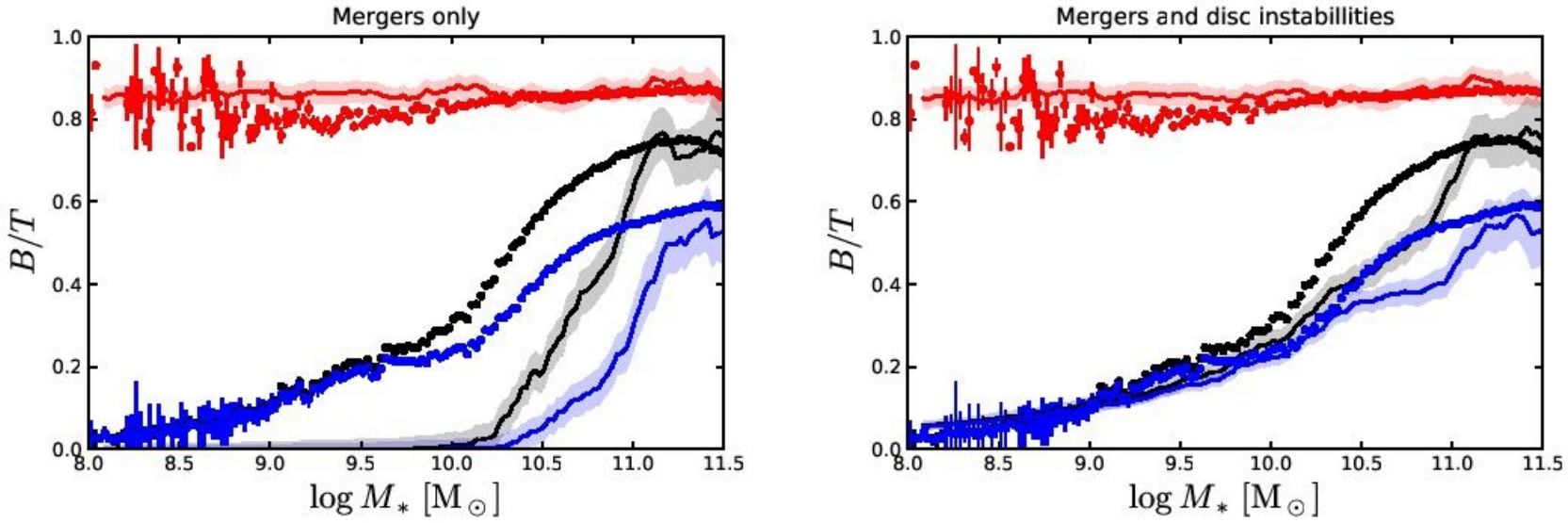

Fig. 10. B/T versus M_* for all galaxies (black), spiral galaxies ($B/T < 0.7$, blue), and elliptical galaxies ($B/T > 0.7$, red). The curves are medians in bins of stellar mass. They refer to GalICS 2.0 without (left) and with (right) disc instabilities. The data points are the observations by Mendel et al. (2014). The width of the shaded areas around the curves shows the standard error on the median.

Усложнение начаных условий

Table 1. Simulations with relaxed initial conditions: parameter values and difference in B/T with respect to the unrelaxed simulations.

λ	$m_{\rm d}$	c	$\Delta\frac{B}{T}$ (%)
0.025	0.01	5	−7
0.025	0.04	5	−17
0.050	0.02	5	+2
0.025	0.01	15	−12
0.025	0.04	15	+7
0.050	0.02	15	−8

Table 2. Simulations with a live halo: parameter values and difference in B/T with respect to those with a static halo.

λ	$m_{\rm d}$	c	$\Delta\frac{B}{T}$ (%)
0.025	0.01	5	+9
0.1	0.04	5	+14
0.025	0.01	10	+7
0.1	0.04	10	+18